PROCEEDINGS OF SPIE

Recent trends in high-resolution hard x-ray tomography

Bert Müller

SPIE.

Recent trends in high-resolution hard X-ray tomography

Bert Müller*a

aBiomaterials Science Center, Department of Biomedical Engineering, University of Basel, 4123 Allschwil, Switzerland

ABSTRACT

Hard X rays are the probe of choice to three-dimensionally visualize optically opaque hard and soft objects as well as their combinations without physical cutting. The currently available methods allow for the quantification of the real and the imaginary parts of local refractive indices. The related phase- and absorption-contrast data are often complementary. The datasets are of GB or TB size due to the object's size and the selected spatial resolution. Therefore the related quantification is challenging. Nevertheless, the current developments pave the way towards imaging larger and larger objects with true micro- and nanometer resolution. Since 1997, the SPIE conference on *Developments in X-ray Tomography*, which was established by U. Bonse, has set the benchmark in the dissemination of knowledge between experts in instrumentation, software development, and a variety of applications. This paper summarizes key aspects of the contributions in the current volume.

Keywords: Hard X ray, computed tomography, phase tomography, microtomography, nanotomography, synchrotron radiation, non-destructive three-dimensional characterization, multi-modal imaging.

1. INTRODUCTION

Hard X-ray tomography belongs to the essentially non-destructive techniques for three-dimensional characterization of a wide variety of objects. It provides three-dimensional data of local refractive indices with isotropic spatial resolution down to the true nanometer scale. Therefore, the related tomographic techniques have become a valuable tool in academia, clinics and industry. Applications range from precision measurements of oral scanners to mummy visualization as well as characterization of the brain tissues in health and disease. The progress of quantitative hard X-ray imaging for this broad palette of applications is intimately related to the advances including powerful X-ray sources and detectors, acquisition protocols for fast and big-data tomograms and the implementation of X-ray optics to reach a spatial resolution below 10 nm. Hardware and software developments enable visualization, artefact removal, and data quantification. Accordingly, the conference was organized in twelve sessions: three on algorithms, four on applications, and five on instrumentation.

A key challenge is to (semi-)automatically analyze the tomographic datasets with sizes in the GB/TB-range. Automatic approaches usually require better contrast than manual procedures. Therefore, artefacts and noise have to be effectively removed. Threshold-based segmentation is often unsatisfactory. Dedicated features have to be defined and identified. Consequently, computational sciences including machine learning and artificial intelligence are increasingly frequent in literature [1]. The participants of the conference incorporated these tools into their reconstruction algorithms and image evaluation.

During the past years, X-ray sources have been developed to bridge the gap between the conventional sources with their restricted flux and the synchrotron radiation facilities with limited accessibility. Liquid metal targets are now established in tomography. Compact light sources are operated similar to a laboratory source, but offer some properties of synchrotron radiation. Especially, the industrial users will appreciate these remarkable developments, because unlike synchrotron radiation facilities, these new X-ray sources can be installed within the company's building and be operated by expert users. Nevertheless, the price for such a device still hinders a wide distribution. The coming years will show how far the price can be reduced and how many academic users can buy such systems.

*bert.mueller@unibas.ch; phone +41 61 207 5430; fax 41 61 207 5499; www.bmc.unibas.ch

2. DEVELOPMENT OF THE PROCEEDINGS PAPERS

2.1 Authors of the proceedings papers

The presenters and authors of the talks, posters and proceedings are experts trained in multiple fields including physics and chemistry, mechanical and electrical engineering, mathematics and computer sciences, medicine and dentistry, biology and geology, *etc*. As a consequence, the general introductions for a broad audience and the numerous details for the specialists are highly appreciated. Thus, we can regard the proceedings as a bargain box for all scientists and engineers working in the fascinating world of X-ray tomography.

Despite the policy of SPIE, not all presenters have submitted a related paper to be included into the current volume. These participants have given several arguments. There is the statement that all relevant information can be found in the recorded presentation and a proceedings paper would be redundant. In fact, eleven out of the twelve talks without conference paper were recorded and available in SPIE's digital database [2-12].

Some authors are afraid that they will be unable to publish their results in a high-ranking journal, once their papers are in the SPIE database. This opinion is hard to understand for the contributors of the current volume. The contributions of the SPIE conference on *Developments in X-ray Tomography XI* from 2017 have been frequently downloaded and cited. The Editors of the present volume are sure that one can always further develop the proceedings paper towards a high-impact journal contribution.

2.2 Chronological development of the proceedings papers

U. Bonse, a prominent pioneer in the field, started the conference series on *Developments in X-ray Tomography* in 1997 and was the responsible Editor for the first five volumes. From 2008 to 2016, S.R. Stock organized five conferences and the related proceedings volumes with 40 to 60 papers each, see Figure 1. In close collaboration with G. Wang and the other members of the program committee, it was my pleasure to organize the reviewing of the accepted posters, oral contributions and submitted manuscripts. The three-day program contained 51 high-level oral presentations and 14 posters, which is reflected in the 51 proceedings papers and 29 recorded presentations of the present volume.
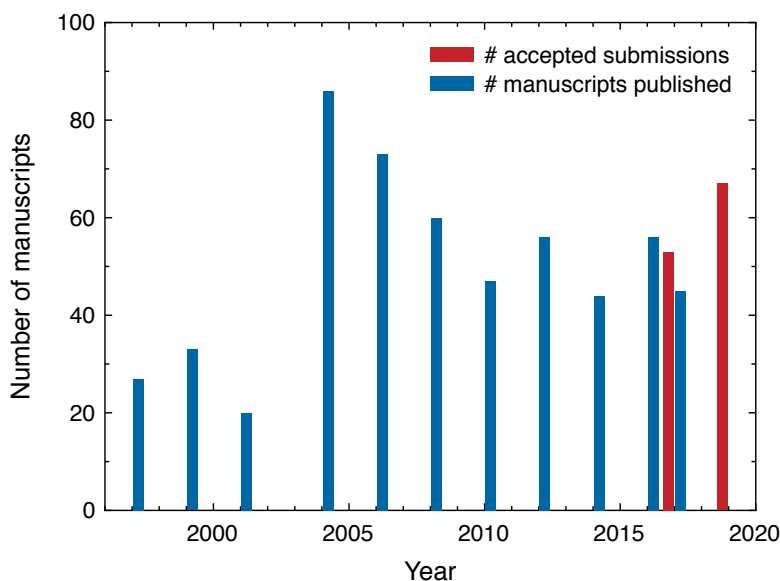

Figure 1. In 1997, the conference series on *Developments in X-ray tomography* was initiated by U. Bonse. He successfully chaired the conference for five times. Subsequently, S.R. Stock chaired the conference for five times as well. The number of manuscripts (blue-colored) in 2017 was 45 out of the 53 presented posters and talks (red-colored). This year, 67 accepted contributions were in the three-day program. In SPIE digital library, Proceedings of SPIE Volume 11113 contains 29 presentations and 51 papers.

3. INSTRUMENTATION

3.1 Synchrotron radiation-based tomography

Synchrotron radiation is known to provide a broad spectrum of hard X rays. Because of the huge flux, one can take advantage of monochromators to tune the wavelength of the photons. For fast imaging, however, the monochromized beam is not intense enough. Therefore, several synchrotron radiation facilities offer pink beams, which originate from the insertion devices and avoid the usage of a monochromator. S. Marathe and coworkers showed how a single harmonic was generated from the undulator at the beamline I13-2, Diamond Light Source, Ditcot, UK [13]. These photons have been used with single-shot grating interferometry to produce three contrast modes, namely absorption, phase, and dark-field imaging. As an example for applications, the authors presented a time series of radiographs recorded during crystallization processes [13].

C. Rau explained that the beamline I13-2, Diamond Light Source, Ditcot, UK is dedicated to multi-scale and multi-modal imaging in real and reciprocal space [14]. It consists of two independently operating experiments for microtomography with in-line phase contrast, for grating interferometry and full-field microscopy, as well as for coherent X-ray diffraction [14]. Therefore, *in situ* and *operando* studies could be carried out, which included examples from carbon dioxide storage, corrosion of steel, mixing of liquids, *etc*. [14].

F. Beckmann showed how the data acquisition time at the high-energy beamline P07, PETRA III, Hamburg, Germany, can be reduced by a factor of two. The synchronized use of two cameras *via* a fast flipping mirror allows for acquisition with one camera, while the second is in the readout mode [15]. This proposition was validated using a miniature lamp and a fossil tooth [15].

At the beamlines ID16B, ESRF Grenoble, France and TOMCAT, Swiss Light Source, Switzerland, fast phase tomography was established to investigate real-time crack formation using 10 Hz rotation and 10 kHz acquisition [16]. C. Le Bourlot and coworkers built a mechanical and temperature environment for tomography experiments [16]. They studied void nucleation, growth and coalescence within intermetallic phases. Digital volume correlation was applied in order to determine the related strain fields. This approach allows for unique experiments of damage evolution in ductile metals.

J. Moosmann and coworkers also developed an *in situ* loading device for tomography at the P07 beamline, PETRA III, Hamburg, Germany [17]. It is also equipped with a temperature control unit that additionally allows controlling the humidity. This additional feature is essential for the study of biodegradable bone implants [17]. The authors showed that they could keep the accumulated dose below 30 kGy. Nevertheless, there are several technical challenges to be mastered. A serious issue, for example, is the beam instability, which probably arose from the monochromator.

High-throughput hard X-ray microscopy and tomography is essential for the progress in the field of life science. Therefore, M. Polikarkov presented the possibilities of the beamline P14, PETRA III, Hamburg, Germany [10]. The X-ray beam yields 6 to 30 keV photons. By means of reflective and refractive optics the beam's shape, size and intensity can be adapted to the desired application. The authors showed fast X-ray tomography of crystals in an optically opaque mesophase with sub-micrometer pixel size [10]. Other applications in collaboration with partners were the visualization of a worm head and pieces of human brain [10].

3.2 Advanced phase tomography

Talbot-Lau interferometry is a powerful X-ray imaging technique with special benefits for low-Z materials. G. Zan and coworkers proposed a microstructured array anode in order to reach a better performance than the combination of extended source plus source grating [18]. The simulations demonstrated that especially at acceleration voltages above 30 kV, the oblique incidence of electrons onto the microstructured transmission target gave rise to a much better photon yield [18].

The research team of A. Momose pushed forward phase tomography using a pink beam extracted by a multilayer mirror at BL28B2, SPring-8, Japan [19]. As phase-stepping is incompatible with fast imaging, the team used the Fourier

transform method or continuous fringe scanning. The power of this four-dimensional imaging was elucidated by a laser ablation study of a carbon-fiber reinforced polymer [19]. This fibrous structure generated dark-field contrast, whose reduction was detected *via* the four-dimensional tomogram. The temporal resolution was optimized toward the sub-second level, which is essential to prevent radiation damages within the polymer matrix [19].

The integration of a grating interferometer into a commercial tomography system was demonstrated previously [20]. Now, the combination of an X-ray microscope with a grating interferometer has been proposed to realize phase tomography with even better spatial resolution. H. Takano presented a Lau interferometer with two gratings, source grating and phase grating, using the incoherent commercial laboratory X-ray source of the ZEISS Xradia 800 Ultra [21]. Using a zone plate between the gratings for self-imaging, tomograms with pixel sizes of 50 nm at a field of view of 65 μm were obtained [21]. Because the conventional deconvolution is unsuitable, the authors employed an iterative algorithm, which drastically reduced the impact of artefacts and noise [21]. They were able to show that several 10 iterations are already sufficient to suitably visualize oral epithelial mucosal cells, polystyrene spheres on plastic fibers using 120 s per 1/360 projections, and a lava tail of a sea skirt [21].

The three-dimensional imaging of the lung in health and disease is a challenge, and the team of K. Morgan has developed experience in taking advantage of using attenuation contrast, phase shifts, and dark-field imaging [22]. The moving organ requires special approaches. The triggered reconstruction, *e.g.* 15 tomograms along one breathing period, is not only possible at a synchrotron radiation facility, but also using the Munich Compact Light Source and a liquid metal source [22]. Therefore, dark-field imaging of cancer and fibrosis for the human lung may become a reality.

3.3 Contrast augmentation in high-resolution hard X-ray tomography

It is well known that staining and embedding of human brain tissues improve the contrast within the brain tissues, see for example [23-26]. The talk of M. Eckermann and the related manuscript [27] highlights the progress in *post mortem* brain imaging. First, the application of staining protocols known from electron microscopy was presented. Second, tomography experiments performed with the liquid-metal jet source at an acceleration voltage of 9.25 keV and a pixel length of 0.54 μm were reported. Third, for higher spatial resolution, the synchrotron facility at GINIX, beamline P10, DESY, Hamburg, Germany was utilized and gave rise to impressive images on the subcellular level concerning the neuronal architecture of the formalin-fixed and paraffin-embedded brain tissue [27].

M. Busse and coworkers also demonstrated how established staining protocols can be applied to stain tissues from biopsies for high-resolution hard X-ray tomographic imaging [28]. Although one can omit X-ray optics, the choice of the source, the sample stage and the detection unit are critical elements to acquire images with sub-micrometer resolution. M. Busse presented the identification of nuclei in liver tissue [28, 29] as a prominent example in current biomedical research.

After the generally expected initial difficulties, the compact light source seems to bridge the gap between the conventional X-ray sources and synchrotron radiation facilities for hard X-ray tomography. This source is based on the inverse Compton scattering. Its energy is tunable between 8 and 42 keV with a spectrum of 3 to 6 % [6]. As B. Hornberger pointed out, the Munich Compact Light Source was utilized for imaging of murine chest, cochlea, coronary angiography, mammography and bone [6].

L. Heck showed how grating-based phase-contrast mammography could benefit from the compact inverse Compton synchrotron source [30]. Using a photon energy of 25 keV and a pixel length of 71 μm, stitching becomes necessary, because the breast is squeezed as per standard practice [30]. Images of freshly dissected mastectomy specimens already showed improved diagnostic content over *ex vivo* clinical mammography images at lower or equal dose [31]. Therefore, it is the goal to realize tomography to reach the density resolution for unique diagnosis.

X. Xi and coauthors investigated the impact of acceleration voltage and beam current of a conventional X-ray source on the contrast and the spatial resolution of low and high density regions of a phantom [32].

3.4 Next-generation components for X-ray tomography

Detection units have plenty of room for improvement, because their efficiency is low compared to other modalities, for example electron microscopy. Another issue relates to the energy resolution of the detectors, which should be developed to provide true spectral scanning. A huge team around P.H. Butler introduced an energy-resolving photon-counting detector that provides five energy channels to be mainly used in medical imaging for selected elements such as calcium in plaque [33]. The authors elucidated the power of their method by visualizing functionalized gold nanoparticles in breast cancer cells [33]. A detailed comparison with the systems of the competitors is still missing.

J.N. Anker demonstrated how X rays enable us to read-out implanted sensors for local pH detection [3]. For example, such a device may be applied to study potential infections around load-bearing implants because we still observe infection near orthopedic implants in a very few percent of the cases [3]. Nevertheless, it remained unclear how the approach can be extended into the third dimension and whether the provided sensitivity can convince the potential users.

J. Gelb from Sigray Inc. proposed the expansion of commercially available high-resolution CT-systems by incorporating sophisticated components [4]. First, the X-ray source was enhanced by replacing the metal target with a diamond target, which exhibited higher thermal conductivity and a micro-structured target, which led to brightness improvement by factors. Second, the X-ray source was complemented using focusing optics, *i.e.* capillary lenses and a Fresnel zone plate. Third, the detection unit included a scintillator-coupled CCD to extend the system to fluorescence and absorption measurements. Finally, the authors briefly described the software package that facilitates the reliable and quick data collection even by newcomers in the field [4].

At the National Institute of Standards and Technology, the team of J.M. LaManna has been developing a unique CT-system for the detection of specific radioactive metals and micrometer-sized features [8]. It should be noted that the NBS-1 photo-neutron source is the primary standard for neutron calibrations in United States. This source, fabricated in 1949, contains the high-Z material radium in a Pt-Ir capsule surrounded by beryllium and needs inspection. J.M. LaManna listed the related challenges in detail and provided proposals for solution [8].

3.5 Enhanced CT systems

A dedicated CT-system was orthogonally placed to a neutron tomography system, so that the simultaneous and complementary data collection became possible [7]. This multimodal facility enabled an efficient three-dimensional registration and subsequently the bivariant histogram analysis [7]. J.M. LaManna impressively demonstrated the analysis of batteries, meteorites, and soil [7]. The soil consisted of sand, water, and air. Whereas the sand is easily detected using X rays, the neutrons are beneficial for the water identification.

The team of M. Lun has introduced X-ray luminescence computed tomography, which combines high-resolution CT with optical imaging [34]. The team summarized the challenges, which included the long acquisition time and limited spatial resolution. In a study involving euthanized mice, they showed how to master these challenges and the current performance of the promising approach. A grid size of 50 μm was selected and a spatial resolution close to 100 μm was reached [34].

Highly X-ray absorbing components are known to create streak artefacts, which compromise the analysis of the interface between metallic implants and the surrounding tissues. M.R. Amma presented an approach to improve the image quality for titanium in calcium solution [35]. This approach is based on energy binning in five ranges, *i.e.* from 7 to 45 keV, from 45 to 55 keV, from 55 to 65 keV, from 65 to 75 keV, and from 75 to 118 keV using the dedicated photon-counting detector. The authors claimed that their instrumentation led to a spatial resolution that is five times better than in clinical CT [35].

The power of conventional X-ray sources is generally thermally limited. Using a liquid-metal target instead of a solid one, the electron flux can be increased by an order of magnitude. Today, several research teams use these liquid-metal jet anodes for tomographic imaging. A. Adibhatla from Excillum Inc. explained how such a source could be reliably operated [2]. The improved brilliance not only allowed for the improvement of the absorption contrast, but also

CT experiments in the phase-contrast mode [2]. The preliminary data could be found on the company's webpage, but still have to be validated. For example, the spot size, which is a crucial parameter, is still not thoroughly characterized.

4. DEVELOPMENT OF ALGORITHMS FOR CT IMAGING AND DATA ANALYSIS

4.1 Image artefact reduction

Although researchers in the field of CT try their best to avoid artefacts, the nature of the sample and the limitations of the CT-system still give rise to a variety of artefacts that compromise the image quality and should be corrected in appropriate manner.

N.T. Vo provided an invited speech on how to tackle the radial lens distortion as well as the irregular detector response and the scattering of scintillation photons. First, the radial lens distortion was corrected using an appropriate grid pattern [36]. Second, the irregular response of the detection system results in sample-dependent ring artefacts. Here, N.T. Vo proposed several procedures, which are implemented in the open-source code [37]. Third, N.T. Vo pointed out that the photon scattering within the detector has impact on phase tomography, but the correction procedure is an ongoing challenge.

Phase wrapping artifacts in grating-based CT are usually avoided by means of a water bath. As pointed out by G. Rodgers and coworkers, omitting the water bath has advantages [38]. Especially for cylindrical samples, one can treat the sinogram and minimize the cupping artefacts [39]. The authors validated the approach for phantoms and a paraffin-embedded mouse brain. The open-source code is now freely available for the community [38].

In CT, the presence of highly X-ray absorbing species leads to streak artifacts. S. Karimi and H. Martz demonstrated that dual-energy CT can reduce these artefacts, but the decomposition is often unstable in the presence of noise [40]. Therefore, they proposed a model-based reconstruction and regression-based sinogram replacement [40]. Applying these algorithms, the imaging data of phantoms and the aluminum objects show less artefacts [40]. Nonetheless, further work has to be invested to better segment the objects of interest [40].

H. Kudo and his team also presented an approach to reduce artefacts from highly X-ray absorbing components within a single step [41]. Now, the authors proposed a fault-tolerant reconstruction algorithm and applied this software to improve the dental imaging data of an entire jaw [42]. They also discussed the application for dark-field imaging and generalized the approach to any other ring artefact correction [42].

Y. Kim won the award for the best poster presentation, which included a cash contribution from the technical sponsor Sigray Inc. This poster and the related paper introduced an image reconstruction algorithm in sparse-view CT [43]. This algorithm is based on a modified nonlocal total variation regularization, Passty's proximal splitting framework, and the selective artefact reduction [43]. The authors demonstrated that reasonable images were reconstructed from 50 to 100 projections with less than 20 iterations [43].

The CT measurements are often time-consuming because a high number of photons has to be detected. Reducing the acquisition time, the data become noisy. Therefore, Y. Teng introduced a reconstruction method on specific smoothing regularizers to suppress the noise and reduce the computational costs [44].

4.2 Compressed sensing and deep learning

A decade ago, Yu and Wang [45] discovered that an exact reconstruction in local tomography has been feasible based on compressed sensing when the object has been piecewise constant over the region of interest. For most cases, however, this assumption is approximate. For medical CT, the images have smooth intensity changes and textures inside the anisotropic tissues. Then, the condition was relaxed for exact local tomography over a piecewise polynomial region of interest [46]. Along this direction, H. Kudo proposed an advanced compressed sensing approach, in which the piecewise constraint has been imposed only over a restricted region, as demonstrated by simulation [47]. It remains to be seen how this approach can be implemented into the experimental studies.

It is a well-established fact that the ionizing radiation associated with CT could induce cancer *via* genetic damage. Therefore, dose reduction is an essential goal of the present research in CT-based medical imaging. H. Xie and coworkers belong to the researchers who wanted to limit the number of radiographs and reconstruct the three-dimensional images for few-view CT [48]. They developed a dual network architecture for reconstructing images directly from a limited number of projections [48]. Their results demonstrated that the dual network architecture produced a competitive performance over some state-of-the-art methods [48].

Deep learning plays an increasing role in the field of medical imaging. F. Fan *et al.* presented an interesting idea by replacing the inner product in the current artificial neuron by a quadratic function for deep learning [49]. In their paper, they prototyped a quadratic residual neural network by incorporating quadratic neurons into a convolutional residual structure, and applied it for metal artifact reduction [49].

CT and magnetic resonance imaging are currently used for diagnoses, treatment planning and even interactive medical interventions. These three-dimensional imaging modalities, however, have limited resolution. In order to improve feature extraction and resolution, one may apply deep learning. In this way, the images can be deblurred, as Q. Lyu *et al.* highlighted [50]. This team suggested an improvement of the resolution by a factor of up to two for both CT and magnetic resonance imaging using the same network architecture [50].

Cone-beam computed tomography could provide three-dimensional breast images, which allow for the detection of sub-millimeter calcifications. The dose, however, has to be kept reasonably small. Therefore, W. Cong *et al.* proposed few-view cone-beam CT through deep-learning-based reconstruction [51]. The results showed that a radiation dose below the threshold set by the Food and Drug Administration is possible for mammographic screening [51].

The poster of J.A. Goldwag and G. Wang and the related 19-page manuscript [52] is a helpful introduction to machine learning in the field.

O. Oh *et al.* applied machine learning for local grating-based phase tomography and claimed that they significantly reduced the artefacts from truncated radiographs [53].

C. You *et al.* successfully used deep convolutional neural networks for the noise reduction in low-dose CT data [54]. They identified more structural details than the counterpart images obtained using state-of-the-art methods [54].

A. Tekawade used convolutional neural networks to evaluate fuel injection data from the Advanced Photon Source at Argonne National Laboratory, Illinois, USA. The segmentation from these CT data was challenging because of numerous artefacts and noise, but by incorporating the two-dimensional convolutional neural network the semi-automatic approach for the surface determination became possible [55].

4.3 Feature extraction

H. Shan and coworkers showed how de-noising supports the conversion of a low-quality to a high-quality image by applying a noderate amount of training datasets [56]. The progressive de-noising became possible in close collaboration with radiologists who were in the loop to train and test. The research team evaluated clinical images from the systems from GE, Philips, and Siemens. Unfortunately, the access to raw data was limited. The algorithms developed and trained were faster and better than the iterative algorithms of these main vendors [56].

Segmenting features from large datasets is time-consuming and a boring procedure. T. Stan gave a speech on the incorporation of convolutional neural networks to reduce segmentation time [57]. As example from materials science, the imaging of dendrites in two binary systems, *i.e.* Pb-Sn and Al-Zn, was selected. Here, the number of training data was small, and the results were not overall satisfying [57]. Nevertheless, the results could guide the development of universal neural networks for segmenting a variety of features, which includes examples from the field of materials science and crystalline growth.

A.P. Cuadros spoke about materials decomposition taking advantage of structured illumination and X-ray filtering using Ce and Dy [58]. This approach was envisioned for the local determination of bone mineralization, breast cancer imaging and water-bone-iodine segmentation [58]. Highly correlated images were obtained from the reconstruction of

energy-binned sinograms [58]. The method, termed compressive spectral X-ray imaging, however, is challenging because one has to solve an ill-posed non-linear problem.

R.A. Ketcham gave an invited talk on the detection of small particles or pores using polychromatic X rays. He started with the segmentation of gold in geology [59] and explained the impact of partial volume phenomena and the blurring. The author proposed a method to successfully compensate partial volume and blurring phenomena by quantifying features that are small in all three dimensions [60]. The method is based on the attenuation anomaly of the small particles.

5. APPLICATIONS

5.1 Three-dimensional imaging: From hard to soft tissues

The crowns of human teeth are highly mineralized, but already small changes in the local mineral concentration can alter the functionality. G.R. Davis talked about the detection of mineralization changes in time using conventional microtomography [61, 62]. Synchrotron radiation is inappropriate as the time scale of mineralization is too slow. One measurement lasted for 24 hours and more [61, 62]. Therefore, the drift - even as small as one pixel - is an issue and needed correction [61]. In order to calibrate the degree of mineralization, a carousel had been employed [61].

The hierarchical structure of bone has been studied for decades. Very recently, the team of H. Birkedal impressively demonstrated the three-dimensional visualization of the osteocyte lacuna-canalicular network using synchrotron radiation [63]. In a first series of experiments, they used the TOMCAT beamline at the Swiss Light Source, Paul Scherrer Institute, Switzerland to obtain the osteocyte lacunae with sub-micrometer voxels sizes [63]. The study of the lacuno-canalicular network in mice was based on holotomography at the beamline ID16, ESRF Grenoble, France. Here, the team recorded data from a piece of bone with a maximal diameter of 400 μm and isotropic voxel sizes of 50 and 130 nm [63, 64].

The same team also provided a speech on the combination of fluorescence and diffraction tomography at the beamline ID13, ESRF Grenoble, France. For specimen preparation, ion beam milling was applied. The related gallium could be found up to a depth of 140 nm [9].

A.-L. Robisch gave a presentation of an extraordinary study of lens-less holographic inline microscopy performed at GINIX setup of the P10 beamline at DESY, Hamburg, Germany [65]. A variety of sub-cellular structures in non-stained human central nervous system's tissue were made visible [26]. The study with 7.0, 7.5 and 8.0 keV photons perfectly combines theory, simulations and experiments [65]. The direct electron density reconstruction based on the contrast transfer function formalism from the holograms recorded at multiple wavelengths is relevant for three-dimensional histopathology with the aim for an improved understanding of Alzheimer disease. The 13-page proceedings contribution [65] was selected as the best paper of the SPIE-conference on *Developments in X-ray Tomography XII* and technically sponsored by Sigray Inc. with a generous cash prize.

The detailed anatomy of animal-microbe symbioses and the spatial distribution of selected elements is essential for the understanding of many phenomena in marine microbiology, environmental sciences and related fields. B. Geier gave an invited talk with a focus on synchrotron radiation-based tomography and subsequent matrix-assisted laser desorption ionization [66]. The tomography data were recorded at the beamline P05, PETRA III, DESY, Hamburg, Germany, which is operated by the Helmholtz-Zentrum Geesthacht, Germany.

5.2 Medically relevant imaging

Chronic kidney disease is prevalent in 15 % of the U.S.-population and 25 % of the population living past 65. Imaging the capillary network using high-resolution hard X-ray tomography is a key to determine the disease-related capillary loss and requires the injection of stains in liquid form. W. Kuo and coworkers have developed a dedicated contrast agent for the visualization of the entire vascular structure of the mouse kidney and compared the results with three-dimensional data of mouse kidneys stained with commercially available contrast agents [67]. The analysis of the results is ongoing and will result in a patent application.

E.-M. Braig elaborated how grating-based phase tomography at the Munich Compact Light Source can be used to decompose the materials in a chicken heart at one selected photon energy [68]. We know that an increasing number of hospitals uses dual-energy CT. The Munich team showed that their approach provides similar representations [68]. The grating-based phase tomography directly and simultaneously yielded the electron density and the X-ray absorption. Their combination allowed for the material decomposition and may become the basis of future diagnostics [68].

The best oral presentation, which was technically sponsored by Sigray with a cash prize, was given by M. Reichardt [69]. He presented a phase tomography study of mouse hearts using the liquid-metal jet source. The data of the entire organ exhibited an effective voxel length close to 5 µm [69]. On the basis of these data and the application of fiber tracking algorithms including principle component analysis, the team could determine the fiber orientation, the degree of filament alignment and the local thicknesses of muscle fiber bundles [69]. This rather surprising result is extremely important for the three-dimensional characterization of tissues, because the human body almost exclusively consists of anisotropic components.

J. Herzen reported on medical applications of laboratory grating-based tomography [5]. She elucidated the combination of the three complementary imaging modes by conventional glass in plastic box with cleaning tissue [5]. The most impressive and relevant data originated from plaque-containing arteries, tumors in liver and kidney, and the decomposition of blood into water and fat [5].

Bone tumors develop in jaw bones and have to be surgically removed. F. Bornert and coworkers pointed out that the combination of cone-beam CT and magnetic resonance imaging is not yet routinely used, although their combination improves the imaging of the interfaces between the bone and the cancerous lesions and therefore the diagnosis and the planning of the interventions [70].

The advanced laboratory system nanotom® m from phoenix x-ray, GE Sensing & Inspection Technologies GmbH, Wunstorf, Germany allows for measurements with true micrometer resolution of objects as large as 10 cm [71]. M. Sacher and coworkers used this approach to determine the accuracy of five current commercial intraoral scanners [72].

H. Wang, a high-school student, *et al.* presented an interesting study aimed at image-quality assessment and data augmentation using reconfigurable mouse phantoms for deep learning [73]. These phantoms were 3D-printed using flexible and rigid materials and contained liquid tissue surrogates to emulate inner organs and body fluids. By means of an energy-discriminating photon-counting CT scanner, the authors identified similarities between the materials used and the mouse tissues [73].

N. Wang, a high-school student, *et al.* showed how a combination of CT and deep learning could support local temperature measurements based on the decreased X-ray absorption due to thermal expansion [74]. This approach is an alternative to the temperature measurements using magnetic resonance imaging, which plays an essential role in focused ultrasound tumor treatments.

5.3 Four-dimensional imaging

Battery research has huge impact on society. I. Zenyuk and coworkers showed how CT became an *operando* technique in investigating the conversion and storage of electrochemical energy [12]. For this purpose, they developed a polymer electrolyte fuel cell compatible with micro- and nanotomography at synchrotron radiation sources. Here, they could discriminate between water and carbon phases [12].

Y. Wu and coworkers introduced grating-based tomography to study cyclic tensile loading of a rubber specimen with 24 Hz repetition rate [75]. With a stroboscopic technique, they smartly combined the phase and dark-field information. The 0.2 s radiographic snapshots were reconstructed, and the obtained three-dimensional data were composed of 65 µm-wide voxels [75]. These results will pave the way to unique three-dimensional imaging of mechanical tests of rather soft materials.

A. Tekawade and coworkers studied the flow within a steel diesel engine by means of synchrotron radiation from the beamline 32-ID at the Advanced Photon Source at Argonne National Laboratory, Illinois, USA [11]. Radiographic

projections, that mainly contained phase information, gathered from repeated injection events with 10,000 frames per second and 2.1 μm pixel size at multiple viewing angles gave rise to a four-dimensional dataset. The necessary photon statistics was obtained by averaging the data from 200 injection events. The data coincided with computational fluid dynamics simulations of the flow profile previously generated for the selected nozzle geometry [11].

5.4 CT of unique objects

Much attention was given to the speech of S.R. Stock, who described the characterization of a mummy [76]. In a first step, the mummy was three-dimensionally imaged using a clinical CT scanner. The obtained dataset guided the diffraction study at the beamline 1-ID of the Advanced Photon Source at Argonne National Laboratory, Illinois, USA. Data were collected at two mummy-detector distances from bones and a highly X-ray absorbing wire. The detected mineral phases corresponded to those of today's human [76]. The study impressively demonstrated that CT-guided, position-resolved diffraction using synchrotron radiation could become a powerful method to non-destructively identify the content of mummies and of other large unique objects.

G. Schulz presented a comprehensive tomography study of hearing and balance organs from 77 ruminants [77]. The three-dimensional data were acquired using the nanotom® m from phoenix x-ray, GE Sensing & Inspection Technologies GmbH, Wunstorf, Germany. The bony labyrinth's lengths were between 7 and 17 mm and correlated with the skull length and the body mass of the species [77]. The early timing of ossification of the bony labyrinth was necessary to achieve the observed negative ontogenetic and evolutionary allometries. Obviously, this relation was critical in the evolution of the diversified hearing and locomotor capacities of mammals.

Silicone can be made so soft that the gravitation force determines the actual shape of the object. J. von Jackowski *et al.* demonstrated that such a soft object with the size of the human jaw could be made visible using the nanotom® m from phoenix x-ray, GE Sensing & Inspection Technologies GmbH, Wunstorf, Germany [78]. The density resolution of the CT-system was insufficient to prove the expected density-stiffness relationship [78]. The successful tomography experiments, however, will allow for finite element modeling to extract the mechanical properties of the silicones used [78].

6. OUTLOOK

It is still meaningful to categorize the developments in X-ray tomography into instrumentation, algorithms and applications, although one always can find overlaps and the assignment to the conference's sessions is somehow arbitrary.

The experimental setups always consist of a more or less sophisticated X-ray source, a rotation stage with several degrees of freedom and micro- or nanometer precision as well as a detection unit with desired dynamic range and spatial and temporal resolution. While the conventional and synchrotron radiation sources are well established, the upcoming liquid metal jet and compact light sources will gain importance in near future. The SPIE-conference on *Developments in X-ray Tomography XII* indicates that the detection units are being constantly updated and more powerful prototypes are conquering the market.

The usage of the reconstruction software available for the commercial systems becomes simpler and simpler. Nonetheless, several teams have implemented additional algorithms for specific applications. During the last two decades, algorithms have become available to correct beam hardening, streak and ring artefacts, phase wrapping *etc*. Such algorithms are the prerequisite for the reasonable solution of segmentation and registration tasks. Very recently, tools known from artificial intelligence and machine learning have been introduced to denoise and deblur the data and to realize automatic segmentation and analysis driven by big data. Here, the progress will proceed in an exponential manner.

The non-destructive three-dimensional imaging plays a vital role in many fields, and it is difficult to predict the growth in the specific areas. Currently, the field is dominated by medical/dental applications, engineering/materials

science applications and cultural heritage. Hierarchical imaging at dedicated instruments will become more important and result in datasets of PB size. Consequently, instrumentation and algorithm developments are critical for the users.

The SPIE-conference series on *Developments in X-ray Tomography* will continue with the 13th edition in August 2021 and follow the lead of the previous editions. Here, the reader is referred to the papers of the Conference Chairs on the trends in micro- and nanotomography using hard X rays [79-83].

ACKNOWLEDGEMENT

REFERENCES

[1] Shan, H., Padole, A., Homayounieh, F., Kruger, U., Khera, R. D., Nitiwarangkul, C., Kalra, M. K., and Wang, G., "Competitive performance of a modularized deep neural network compared to commercial algorithms for low-dose CT image reconstruction," Nature Machine Intelligence **1**(6), 269-276 (2019).

[2] Adibhatla, A., Takman, P., Larsson, D., and Lundstrom, U., "Use of liquid MetalJet sources in applications of biomedical imaging and computed tomography (Conference Presentation)," Proc. SPIE **11113**, 111131E (2019).

[3] Anker, J. N., "Implanted sensors to measure pH and other analytes with x-ray readout (Conference Presentation)," Proc. SPIE **11113**, 111130D (2019).

[4] Gelb, J., Vine, D., Qiao, R., Yang, X., Seshadri, S., Stripe, B., Lewis, S., Lau, S. H., and Yun, W., "The new x-ray laboratory: enabling access to structure, composition, and morphology through laboratory x-ray instrumentation (Conference Presentation)," Proc. SPIE **11113**, 111130E (2019).

[5] Herzen, J., "High-sensitivity quantitative x-ray phase-contrast computed tomography for biomedical applications (Conference Presentation)," Proc. SPIE **11113**, 111130T (2019).

[6] Hornberger, B., Kasahara, J., and Gifford, M., "A compact light source for x-ray tomography applications across length scales (Conference Presentation)," Proc. SPIE **11113**, 111130L (2019).

[7] LaManna, J. M., Hussey, D. S., Baltic, E., and Jacobson, D. L., "Analysis algorithms for simultaneous neutron and x-ray tomography datasets from the NIST NeXT system (Conference Presentation)," Proc. SPIE **11113**, 111131C (2019).

[8] LaManna, J. M., Mumm, H. P., and Dewey, M. S., "X-ray tomography of internal components of the NBS-1 photo-neutron source (Conference Presentation)," Proc. SPIE **11113**, 111130F (2019).

[9] Palle, J., Kølln Wittig, N., Grünewald, T., Kubec, A., Rosenthal, M., and Birkedal, H., "Combined fluorescence and diffraction tomography of bone at <140-nm resolution (Conference Presentation)," Proc. SPIE **11113**, 1111305 (2019).

[10] Polikarpov, M., Bourenkov, G., Snigirev, A., and Schneider, T., "High-throughput x-ray imaging, microscopy, and tomography for biological applications on EMBL beamline P14 at PETRA III (Conference Presentation)," Proc. SPIE **11113**, 1111307 (2019).

[11] Tekawade, A., Sforzo, B. A., Matusik, K. E., Kastengren, A. L., and Powell, C. F., "Application of synchrotron x-ray imaging and micro-CT to 4D visualization of multiphase flow inside a steel fuel nozzle (Conference Presentation)," Proc. SPIE **11113**, 1111310 (2019).

[12] Zenyuk, I., Shum, A., Leonard, E., De Andrade, V., Parkinson, D., and Xiao, X., "Operando multimodal x-ray tomography of transport in electrochemical energy-conversion and storage devices (Conference Presentation)," Proc. SPIE **11113**, 111130Y (2019).

[13] Marathe, S., Storm, M., Kuppili, V. S. C., Harrison, R., Das, G., Schroeder, S. L. M., Cipiccia, S., Döring, F., David, C., and Rau, C., "Development of synchrotron pink beam X-ray grating interferometer for fast imaging and tomography applications," Proc. SPIE **11113**, 1111319 (2019).

[14] Rau, C., Storm, M., Marathe, S., Bodey, A. J., Zdora, M., Cipiccia, S., Batey, D., Shi, X., Schroeder, S. M. L., Das, G., Loveridge, M., Ziesche, R., and Connolly, B., "Fast Multi-scale imaging using the Beamline I13L at the Diamond Light Source," Proc. SPIE **11113**, 111130P (2019).

[15] Beckmann, F., Hammel, J. U., Moosmann, J., Lottermoser, L., Gunnell, G. F., and Habersetzer, J., "Optimization of high-energy microtomography using synchrotron radiation at PETRA III," Proc. SPIE **11113**, 111131A (2019).

[16] Le Bourlot, C., Azman, A., Adrien, J., and Maire, E., "An example of in situ ductile damage analysis by tracking algorithm," Proc. SPIE **11113**, 1111317 (2019).

[17] Moosmann, J., Wieland, D. C. F., Zeller-Plumhoff, B., Galli, S., Krüger, D., Ershov, A., Lautner, S., Sartori, J., Dean, M., Köhring, S., Burmester, H., Dose, T., Peruzzi, N., Wennerberg, A., Willumeit-Römer, R., Wilde, F., Heuser, P., Hammel, J. U., and Beckmann, F., "A load frame for in situ tomography at PETRA III," Proc. SPIE **11113**, 1111318 (2019).

[18] Zan, G., Vine, D. J., S.J.Y., L., Wang, Q., Yun, W., and Wang, G., "Systematic analysis of microstructured array anode target for hard x-ray grating interferometer," Proc. SPIE **11113**, 111130H (2019).

[19] Momose, A., Vegso, K., Takano, H., Wu, Y., Hashimoto, K., and Hoshino, M., "Four-dimensional pink-beam x-ray phase tomography for studying laser processing," Proc. SPIE **11113**, 111130I (2019).

[20] Khimchenko, A., Schulz, G., Thalmann, P., and Muller, B., "Implementation of a double-grating interferometer for phase-contrast computed tomography in a conventional system nanotom((R)) m," APL Bioeng **2**(1), 016106 (2018).

[21] Takano, H., Hashimoto, K., Nagatani, Y., Wu, Y., and Momose, A., "Development of laboratory-based x-ray phase tomographic microscope," Proc. SPIE **11113**, 11113J (2019).

[22] Morgan, K., Gradl, R., Dierolf, M., Jud, C., Günther, B., Werdiger, F., Gardner, M., Cmielewski, P., McCarron, A., Farrow, N., Haas, H., Kimm, M. A., Yang, L., Kutschke, D., Stoeger, T., Schmid, O., Achterhold, K., Pfeiffer, F., Parsons, D., and Donnelley, M., "In vivo x-ray imaging of the respiratory system using synchrotron sources and a compact light source," Proc. SPIE **11113**, 111130G (2019).

[23] Hieber, S. E., Bikis, C., Khimchenko, A., Schweighauser, G., Hench, J., Chicherova, N., Schulz, G., and Muller, B., "Tomographic brain imaging with nucleolar detail and automatic cell counting," Sci Rep **6**, 32156 (2016).

[24] Khimchenko, A., Bikis, C., Pacureanu, A., Hieber, S. E., Thalmann, P., Deyhle, H., Schweighauser, G., Hench, J., Frank, S., Muller-Gerbl, M., Schulz, G., Cloetens, P., and Muller, B., "Hard X-Ray Nanoholotomography: Large-Scale, Label-Free, 3D Neuroimaging beyond Optical Limit," Adv Sci (Weinh) **5**(6), 1700694 (2018).

[25] Khimchenko, A., Deyhle, H., Schulz, G., Schweighauser, G., Hench, J., Chicherova, N., Bikis, C., Hieber, S. E., and Muller, B., "Extending two-dimensional histology into the third dimension through conventional micro computed tomography," Neuroimage **139**, 26-36 (2016).

[26] Topperwien, M., van der Meer, F., Stadelmann, C., and Salditt, T., "Three-dimensional virtual histology of human cerebellum by X-ray phase-contrast tomography," Proc Natl Acad Sci U S A **115**(27), 6940-6945 (2018).

[27] Eckermann, M., Töpperwien, M., Ruhwedel, T., Möbius, W., and Salditt, T., "Evaluation of different heavy-metal stains and embedding media for phase contrast tomography of neuronal tissue," Proc. SPIE **11113**, 111130N (2019).

[28] Busse, M., Ferstl, S., Müller, M., Kimm, M. A., Drecoll, E., Bürkner, T., Allner, S., Hehn, L., Dierolf, M., Achterhold, K., Herzen, J., Pfeiffer, D., Rummeny, E. J., Weichert, W., and Pfeiffer, F., "New staining tools and developments for 3D soft tissue CT imaging," Proc. SPIE **11113**, 111130O (2019).

[29] Muller, M., Kimm, M. A., Ferstl, S., Allner, S., Achterhold, K., Herzen, J., Pfeiffer, F., and Busse, M., "Nucleus-specific X-ray stain for 3D virtual histology," Sci Rep **8**(1), 17855 (2018).

[30] Heck, L., Eggl, E., Grandl, S., Dierolf, M., Jud, C., Günther, B., Achterhold, K., Mayr, D., Gleich, B., Hellerhoff, K., Pfeiffer, F., and Herzen, J., "Dose and spatial resolution analysis of grating-based phase-contrast mammography using an inverse Compton x-ray source," Proc. SPIE **11113**, 111130M (2019).

[31] Eggl, E., Grandl, S., Sztromicronkay-Gaul, A., Dierolf, M., Jud, C., Heck, L., Burger, K., Gunther, B., Achterhold, K., Mayr, D., Wilkens, J. J., Auweter, S. D., Gleich, B., Hellerhoff, K., Reiser, M. F., Pfeiffer, F., and Herzen, J., "Dose-compatible grating-based phase-contrast mammography on mastectomy specimens using a compact synchrotron source," Sci Rep **8**(1), 15700 (2018).

[32] Xi, X., Sun, Z., Han, Y., Li, L., Yan, B., and Li, Y., "Effect of tube setting variables on image quality in industrial x-ray computed tomography," Proc. SPIE **11113**, 111131U (2019).

[33] Butler, P. H., Adebileje, S. A., Alexander, S. D., Amma, M. R., Amjomrouz, M., Asghariomabad, F., Atharifard, A., Atlas, J., Bamford, B., Bell, S. T., Bheesette, S., Butler, A. P. H., Carbonez, P., Chambers, C., Chernoglazov, A. I., Dahal, S., Damet, J., de Ruiter, A., Doesburg, R. M. N., Duncan, N., Gieseg, S. P., Goulter, B. P., Gurney, S., Healy, J. L., Kanithi, P., Kirkbride, T., Lansley, S. P., Lowe, C., Mandalika, V. B. H., Marfo, E., Matanaghi, A., Moghiseh, M., Palmer, D., Panta, R. K., Prebble, H. M., Raja, A. Y., Sayous, Y., Renaud, P., Schleich, N., Searle, E., Sheeja, J. S., Uddin, R., Vanden Broeke, L., Vivek , V. S., Walker, E. P., Walsh, M. F., Wijesooriya, M., and Younger, W. R., "MARS pre-clinical imaging: the benefits of small pixels and good energy data," Proc. SPIE **11113**, 111130C (2019).

[34] Lun, M. C., and Li, C., "Focused x-ray luminescence computed tomography," Proc. SPIE **11113**, 111131B (2019).

[35] Amma, M. R., Butler, A. P. H., Raja, A. Y., Bamford, B., Butler, P., Walker, E. P., Matanaghi, A., Adebileje, S. A., Anderson, N., Anjomrouz, M., Asghariomabad, F., Atharifard, A., Bell, S. T., Bheesette, S., Chernoglazov, A. I., Dalefield, T., de Ruiter, N. J. A., Duncan, N., Doesburg, R. M. N., Gieseg, S., Goulter, B. P., Alexander, S. D., Gurney, S., Healy, J. L., Hilton, P. J., Dahal, S., Carbonez, P., Damet, J., Chambers, C., Kanithi, P., Kirkbride, T., Lansley, S. P., Lowe, C., Mandalika, V. B. H., Marfo, E., Moghiseh, M., Palmer, D., Panta, R. K., Prebble, H. M., Ramyar, M., Renaud, P., Schleich, N., Searle, E., Shamshad, M., Sheeja, J. S., Uddin, R., Vanden Broeke, L., Vivek, V. S., Wijesooriya, M., Walsh, M. F., Baer, K., Tredinnick, S., and Woodfield, T., "Assessment of metal implant induced artefacts using photon counting spectral CT," Proc. SPIE **11113**, 111131D (2019).

[36] Vo, N. T., Atwood, R. C., and Drakopoulos, M., "Radial lens distortion correction with sub-pixel accuracy for X-ray micro-tomography," Opt. Express **23**(25), 32859-32868 (2015).

[37] Vo, N. T., Atwood, R. C., and Drakopoulos, M., "Preprocessing techniques for removing artifacts in synchrotron-based tomographic images," Proc. SPIE **11113**, 111131I (2019).

[38] Rodgers, G., Schulz, G., Deyhle, H., Marathe, M., Bikis, C., Müller, B., and Weitkamp, T., "Correction of phase wrapping artifacts in grating-based hard x-ray tomography," Proc. SPIE **11113**, 1111308 (2019).

[39] Rodgers, G., Schulz, G., Deyhle, H., Marathe, S., Bikis, C., Weitkamp, T., and Müller, B., "A quantitative correction for phase wrapping artifacts in hard X-ray grating interferometry," Applied Physics Letters **113**(9), 093702 (2018).

[40] Karimi, S., and Martz, H., "Regression-based sinogram replacement for CT metal artifact reduction," Proc. SPIE **11113**, 1111309 (2019).

[41] Kudo, H., Takaki, K., Yamazaki, F., and Nemoto, T., "Proposal of fault-tolerant tomographic image reconstruction," Proc. SPIE **9967**, 99671K (2016).

[42] Kudo, H., Dong, J., Chigita, K., and Kim, Y., "Metal artifact reduction in CT using fault-tolerant image reconstruction," Proc. SPIE **11113**, 111130A (2019).

[43] Kim, Y., Kudo, H., Chigita, K., and Lian, S., "Image reconstruction in sparse-view CT using improved nonlocal total variation regularization," Proc. SPIE **11113**, 111131K (2019).

[44] Teng, Y., Guo, Q., and Wang, G., "Smoothing L0- and L1-Norm regularizers and their relations to non-local means for CT reconstruction," Proc. SPIE **11113**, 111131M (2019).

[45] Yu, H., and Wang, G., "Compressed sensing based interior tomography," Phys Med Biol **54**(9), 2791-2805 (2009).

[46] Wang, G., and Yu, H., "The meaning of interior tomography," Phys Med Biol **58**(16), R161-R186 (2013).

[47] Kudo, H., "Advanced compressed sensing image reconstruction for interior tomography," Proc. SPIE **11113**, 111130U (2019).

[48] Xie, H., Shan, H., Cong, W., Zhang, X., Liu, S., Ning, R., and Wang, G., "Dual network architecture for few-view CT - trained on ImageNet data and transferred for medical imaging," Proc. SPIE **11113**, 111130V (2019).

[49] Fan, F., Shan, H., Gjesteby, L., and Wang, G., "Quadratic neural networks for CT metal artifact reduction " Proc. SPIE **11113**, 111130W (2019).

[50] Lyu, Q., You, C., Shan, H., Zhang, Y., and Wang, G., "Super-resolution MRI and CT through GAN-CIRCLE," Proc. SPIE **11113**, 111130X (2019).

[51] Cong, W., Shan, H., Zhang, X., Liu, S., Ning, R., and Wang, G., "Deep-learning-based breast CT for radiation dose reduction," Proc. SPIE **11113**, 111131L (2019).

[52] Goldwag, J. A., and Wang, G., "Training artificial neurons: an introduction to machine learning," Proc. SPIE **11113**, 111131P (2019).

[53] Oh, O., Wang, G., and Lee, S. W., "Machine learning assisted interior phase contrast CT," Proc. SPIE **11113**, 111131R (2019).

[54] You, C., Yang, L., Zhang, Y., and Wang, G., "Low-dose CT via deep CNN with skip connection and network-in-network," Proc. SPIE **11113**, 111131W (2019).

[55] Tekawade, A., Sforzo, B. A., Matusik, K. E., Kastengren, A. L., and Powell, C. F., "High-fidelity geometry generation from CT data using convolutional neural networks," Proc. SPIE **11113**, 111131X (2019).

[56] Shan, H., Jia, X., Mueller, K., Kruger, U., and Wang, G., "Low-dose CT simulation with a generative adversarial network," Proc. SPIE **11113**, 111131F (2019).

[57] Stan, T., Thompson, Z. T., and Voorhees, P. W., "Building towards a universal neural network to segment large materials science imaging datasets," Proc. SPIE **11113**, 111131G (2019).

[58] Cuadros, A. P., Ma, X., and Arce, G. R., "Compressive x-ray material decomposition using structured illumination," Proc. SPIE **11113**, 111131H (2019).

[59] Ketcham, R. A., and Mote, A. S., "Accurate Measurement of Small Features in X-Ray CT Data Volumes, Demonstrated Using Gold Grains," Journal of Geophysical Research: Solid Earth **124**(4), 3508-3529 (2019).

[60] Ketcham, R. A., "Resolution-invariant measurements of small objects in polychromatic CT data," Proc. SPIE **11113**, 11113B (2019).

[61] Davis, G., "Time-lapse x-ray microtomography for detecting small changes in local mineral concentration," Proc. SPIE **11113**, 1111315 (2019).

[62] Davis, G. R., Mills, D., and Anderson, P., "Real-time observations of tooth demineralization in 3 dimensions using X-ray microtomography," J Dent **69**, 88-92 (2018).

[63] Palle, J., Wittig, N. K., Østergaard, M., Jensen, A. B., and Birkedal, H., "The osteocyte lacuno-canalicular network in bone investigated by synchrotron tomographies," Proc. SPIE **11113**, 1111316 (2019).

[64] Wittig, N. K., Laugesen, M., Birkbak, M. E., Bach-Gansmo, F. L., Pacureanu, A., Bruns, S., Wendelboe, M. H., Bruel, A., Sorensen, H. O., Thomsen, J. S., and Birkedal, H., "Canalicular Junctions in the Osteocyte Lacuno-Canalicular Network of Cortical Bone," ACS Nano **13**(6), 6421-6430 (2019).

[65] Robisch, A.-L., Eckermann, M., Töpperwien, M., van der Meer, F., Stadelmann, C., and Salditt, T., "Nanoscale x-ray holo-tomography of human brain tissue with phase retrieval based on multiphoton energy recordings," Proc. SPIE **11113**, 1111304 (2019).

[66] Geier, B., Franke, M., Ruthensteiner, B., González Porras, M. A., Gruhl, A., Wörmer, L., Moosmann, J., Hammel, J. U., Dubilier, N., Leisch, N., and Liebeke, M., "Correlative 3D anatomy and spatial chemistry in animal-microbe symbioses: developing sample preparation for phase-contrast synchrotron radiation based microcomputed tomography and mass spectrometry imaging," Proc. SPIE **11113**, 1111306 (2019).

[67] Kuo, W., Schulz, G., Müller, B., and Kurtcuoglu, V., "Evaluation of metal nanoparticle- and plastic resin-based x-ray contrast agents for kidney capillary imaging," Proc. SPIE **11113**, 111130Q (2019).

[68] Braig, E.-M., Dierolf, M., Guenther, B., Mechlem, K., Allner, S., Sellerer, T., Achterhold, K., Gleich, B., Rummeny, E., Pfeiffer, D., Pfeiffer, F., and Herzen, J., "Single-energy material decomposition with grating-based x-ray phase-contrast CT," Proc. SPIE **11113**, 111130R (2019).

[69] Reichardt, M., Töpperwien, M., Khan, A., Alves, F., and Salditt, T., "Fiber orientation in a whole mouse heart reconstructed by laboratory phase-contrast micro-CT," Proc. SPIE **11113**, 111130S (2019).

[70] Bornert, F., Gros, C.-I., Lutz, J.-C., Schultz, D., Riehm, S., Choquet, P., Schulz, G., Müller, B., and Dillenseger, J.-P., "Cone-Beam Computed Tomography - Magnetic Resonance Imaging registration in dento-maxillary imaging," Proc. SPIE **11113**, 111131N (2019).

[71] Vögtlin, C., Schulz, G., Jäger, K., and Müller, B., "Comparing the accuracy of master models based on digital intra-oral scanners with conventional plaster casts," Physics in Medicine **1**, 20-26 (2016).

[72] Sacher, M., Schulz, G., Deyhle, H., Jäger, K., and Müller, B., "Comparing the accuracy of intraoral scanners, using advanced micro computed tomography," Proc. SPIE **11113**, 111131Q (2019).

[73] Wang, H., Li, M., Getzin, M., Arduini, B. L., Covert, N., Vashishth, D., and Fitzgerald, P., "Deformable and reconfigurable mouse phantoms with 3D printing and LTS technologies," Proc. SPIE **11113**, 111131S (2019).

[74] Wang, N., Li, M., Shan, H., and Yan, P., "Deep learning based CT thermometry for thermal tumor ablation," Proc. SPIE **11113**, 111131T (2019).

[75] Wu, Y., Takano, H., and Momose, A., "Development of grating interferometer-based stroboscopic X-ray tomography," Proc. SPIE **11113**, 111130Z (2019).

[76] Stock, S. R., Stock, M. K., and Almer, J. D., "In situ position-resolved x-ray diffraction of an intact Roman-era Egyptian mummy guided by computed tomography," Proc. SPIE **11113**, 1111312 (2019).

[77] Costeur, L., Mennecart, B., Müller, B., and Schulz, G., "Observations on the scaling relationship between bony labyrinth, skull size and body mass in ruminants," Proc. SPIE **11113**, 1111313 (2019).

[78] von Jackowski, J., Schulz, G., Töpper, T., Osmani, B., and Müller, B., "Three-dimensional characterization of soft silicone elements for intraoral device," Proc. SPIE **11113**, 1111314 (2019).

[79] Stock, S. R., "Trends in micro- and nanoComputed Tomography 2008-2010," Proc. SPIE **7804**, 780402 (2010).

[80] Stock, S. R., "Trends in micro- and nanoComputed Tomography 2010-2012," Proc. SPIE **8506**, 850602 (2012).

[81] Stock, S. R., "Trends in micro- and nano-computed tomography 2012-2014," Proc. SPIE **9212**, 921202 (2014).

[82] Stock, S. R., "Developments in X-ray Tomography I - IX," Proc. SPIE **9967**, 996702 (2016).

[83] Müller, B., "Recent trends in high-resolution X-ray tomography " Proc. SPIE **10391**, 1039102 (2017).